Quantification and comparison of the reaction properties of FEBEX and MX-80 clays with saponite, as immobilizers of europium under subcritical conditions.

María Villa-Alfageme[1,*], Santiago Hurtado[2], Miguel A. Castro[3], Said El Mrabet[3], M. Mar Orta[3], M. Carolina Pazos[3], María D. Alba[3]

[1]Dpto. Física Aplicada II, Universidad de Sevilla

[2]Centro de Investigación, Tecnología e Innovación CITIUS. Universidad de Sevilla

[3]Instituto Ciencia de los Materiales de Sevilla (CSIC-US)

* Corresponding author: e-mail: mvilla@us.es (M. Villa-Alfageme)

Abstract

The evaluation of the retention mechanisms in FEBEX and MX-80 bentonites, selected as reference materials to construct engineered barriers, carries major implications in the safe storage of nuclear waste. The kinetics and reactivity of the reaction of Eu -as a lanthanide high-level radioactive waste simulator- with FEBEX and MX-80 were investigated, in addition to their immobilisation capacity through a recently discovered chemical retention mechanism and the structural analysis of the reaction products. Hydrothermal treatments were accomplished with $Eu(NO_3)_3$ (^{151}Eu and ^{153}Eu, with 52.2% ^{153}Eu) and spiked with radioactive ^{152}Eu for the quantification of the reactions. Results were compared with saponite as the reference smectite. The strong dependence of the reaction parameters with temperature and time was quantified and the reaction velocity was evaluated. The velocity follows these trends: 240 days are needed for the total retention of europium for temperatures over 200ºC; below 150ºC, significantly longer reaction times, on the order of three years are required to complete the reaction. Clays do not

influence velocity rates, but the retention capacity of bentonites remains lower than for saponite. At 300ºC, the milliequivalents retained by the three clays are consistently over CEC. The structural analyses reveal not only adsorption of europium but also the presence of $Eu(OH)_3$ precipitation and Eu_2SiO_3 confirming the existence of a chemical reaction.

Key Words: Bentonite, smectite, disilicates, europium, hydrothermal treatment, radioactive waste.

1. Introduction

In many countries, the development of Deep Geological Repositories (DGR), for the storage of high-level radioactive waste (HLRW) is based on a system of multiple barriers. Most safety within the repositories relies on the engineered barrier (Savage and Chapman, 1982). Clays present low permeability, and high sorption and swelling capacity, which makes them ideal materials for natural and engineered barriers for nuclear waste isolation (Pusch, 2006). A clay barrier is able to delay the diffusion and immobilise, in certain experimental conditions, the radioactive wastes through a physical-chemical mechanism, such as adsorption, desorption or even a chemical reaction including the formation of secondary stable mineral phases. At the present time, bentonite is accepted as the most suitable clay for the engineered barrier in DGRs (Fernandes et al., 2012).

The performance of clay as the main component of the engineered barrier in the DGR has been intensively studied, e.g. its response to intense irradiation (Sorieul et al., 2008), its sorption properties (Fernandes et al., 2012; Stumpf et al., 2001), colloid formation reactions (Bouby et al., 2011) and the connections between sorption chemistry and mechanical compaction (Miller and Wang, 2012). Regarding the clay adsorption properties, recent studies highlight the existence of an additional retention mechanism (Alba et al., 2009a; Trillo et al., 1994). The systematic study

of the interaction of the Rare Earth Element (REE) cations, such as La, Lu, Nd, Sm, as actinides chemical analogues, with natural and artificial clay minerals, reveal a reaction mechanism, based on the chemical interaction between the lanthanide cations and the orthosilicate anions of the lamellar structure (Alba et al., 2011; Alba and Chain, 2005). At subcritical conditions, (temperature and pressure), an insoluble and chemically stable phase, $REE_2Si_2O_7$, is generated (Alba et al., 2009b). Therefore, the expected retention capacity of bentonite increases and can provide a stable immobilisation mechanism even when its sorption and swelling capacities fail (Alba and Chain, 2007).

These previous studies are focused on the structural analysis of $REE_2Si_2O_7$, after the hydrothermal reaction between REE cations and clay minerals (Alba and Chain, 2005; Alba and Chain, 2007; Alba et al., 2009a). More recently, Alba et al., (2011) have quantified the Eu^{3+} immobilization by a standard saponite, and physical and chemical interactions are analysed. However, the final motivation of these analyses is the study of bentonites, since they constitute one of the most recommended materials for the construction of the engineered barrier.

In this work, an evaluation of the retention mechanisms in bentonites is performed. The FEBEX and MX-80 clays are commonly selected as reference materials by various nuclear waste management agencies in the construction of engineered barriers in a potential DGR (Villar et al., 2012).

Therefore, the aims of this study are: i) quantification of the immobilisation power of the bentonites FEBEX and MX-80 in comparison with the pure smectite saponite; ii) completion of a kinetic analysis of the process and a structural analysis of the products of reaction; and iii) verification of the mechanism in a wide range of temperatures, including those where the extent of the reaction is so low that is not possible to detect structural changes.

In order to achieve these objectives, hydrothermal treatments of FEBEX and MX-80 with stable europium are performed in the temperature range between 80ºC and 300ºC. Stable europium was spiked with ^{152}Eu in order to quantitatively compare the reactivity and kinetics of the bentonites to the saponite.

2. Materials and methods

2.1. Clay samples.

The FEBEX bentonite was extracted from the Cortijo de Archidona deposit (Almería, Spain). The processing at the factory consisted of disaggregation and gently grinding, drying at 60 °C and sieving by 5mm (ENRESA, 2000; ENRESA, 2006). The montmorillonite content of the FEBEX bentonite was above 90% (92±3%)(Villar et al., 2012). The MX-80 bentonite was extracted from Wyoming (USA) and was supplied in the form of powder homoionised with sodium (Madsen, 1998). The MX-80 batch used in this investigation was mainly composed of montmorillonite (83%)(Villar et al., 2012). As reference, a purified saponite from the Source Clay Minerals Repository of the University of Missouri (Columbia) was used as reference material (Alba et al., 2001). Table 1 summarizes the main clay characteristics (Galunin et al., 2010).

2.2. Eu^{3+} solutions.

Two sets of starting solutions of $7.9 \cdot 10^{-2}$M $Eu(NO_3)_3$ (^{151}Eu and ^{153}Eu, with 52.2% ^{153}Eu) were prepared: The first solution contained solely stable Eu isotopes; the second solution was enriched with the radioisotope ^{152}Eu (with a half-life of 13.5 years). A volume of 1 ml from a diluted standard solution up to a total activity of 9.8 Bq was added to 35 ml of the former

95 solution, as a compromise for safe radioactive handling and high counting rates for fast
96 measurements. That activity corresponded to 10^{-14} mol of ^{152} Eu. The pH of the two solutions was
97 adjusted to pH=6.0-6.5, by slowly adding 0.05 M ammonia solution while stirring.
98
99 *2.3. Hydrothermal treatments.*
100 Three hundred milligrams of the powdered samples (Saponite, FEBEX, MX-80) were
101 dispersed in the 40 ml of Eu^{3+} solutions and were heated in a stainless steel reactor (Perdigón,
102 2002), at the temperatures and times summarized in Table 2. The cells marked with vertical lines
103 correspond to the treatment with a starting solution of $7.9 \cdot 10^{-2}$M $Eu(NO_3)_3$, while the grey cells
104 correspond to the treatment with a starting solution of $7.9 \cdot 10^{-2}$M $Eu(NO_3)_3$ enriched with the
105 ^{152}Eu isotope. The reaction products were collected by filtering using a Millipore filter with 0.45
106 μm pore diameter, washed with distilled water, and dried in air at 60ºC. The reaction solution and
107 the washing liquid were kept for quantitative analysis of europium by gamma spectroscopy. The
108 solid samples were collected either for gamma (^{152}Eu spiked), or for structural analysis by XRD
109 and SEM/EDX (not spiked with radioactive isotopes).
110
111 *2.4. Characterization methods.*
112 A Canberra, hyper-pure n-type germanium gamma detector (HPGe), was used for ^{152}Eu
113 gamma spectrometry measurements, in Radioisotopes Service at CITIUS laboratories
114 (Universidad de Sevilla). Counting efficiency was experimentally determined by means of
115 preparing standards spiked with^{152}Eu for the two geometries analysed: filter and cylindrical
116 beaker. Efficiency was verified for both counting geometries using Monte Carlo simulations,
117 through an optimized LABSOCS program (Hurtado and Villa, 2010).

In the structural study, powered non-^{152}Eu spiked samples were analysed using a Bruker D8 to obtain an X-Ray diffraction diagram (XRD), also located at CITIUS laboratories (Universidad de Sevilla). Radiation of Cu, Kα, and Ni filters was chosen, whereby 40 kV, 40 mA, 0.05º 2θ step, and 3 s counting time were the operational parameters. Crystalline phase identification was carried out using the DIFFRAC^{plus} Evaluation package (©2010 Bruker AXS GmbH, Karlsruhe, Germany).

When crystalline phases could not be identified by XRD, scanning electron microscopy (SEM/EDX) was chosen. Morphologies and chemical compositions were analysed in Microscopy Service in ICMS (CSIC-Universidad de Sevilla) with a SEM-FEG HITACHI S- 4800; a scanning electron microscope equipped with an Xflash 4010 (Bruker) for energy dispersive X-ray (EDX) analysis.

3. Results and discussion

3.1. Quantification of the reactivity of clays with Eu^{3+}.

Retention of europium in the bentonites was evaluated from the comparison of the initially added radioactive europium with the measurement of the europium in the filter after hydrothermal treatment. Subsequently, milliequivalents of europium per 100g clay retained in the solid were calculated and displayed for every hydrothermal treatment in Fig. 1, where the amount of europium that would be needed to satisfy the CEC (Cation Exchange Capacity) of the clays (horizontal lines) is also shown.

Predominantly, when the reaction temperature increases, the amount of europium retained in the solid phase increases. At the beginning of the reaction (t=0), the milliequivalents of europium retained by the clays were within the range of the CEC for every temperature, that is, the

europium was retained exclusively due to cationic exchange, and no significant chemical reaction took place. At 300ºC, for longer reaction times, regardless of the clay, the milliequivalents of retained europium were higher than the CEC, that is, immobilization was not only associated to sorption in specific and non-specific sites, but also to the chemical reaction between europium and the clay framework. For the FEBEX and MX-80 bentonites, the amount of europium retained, although higher than CEC, was significantly lower than for saponite. At 150º C, only saponite was able to retain europium above its CEC, and hence the immobilization of europium in FEBEX and MX-80 is associated exclusively to CEC for the first two months of the reaction. At 80ºC, no clay was able to retain milliequivalents of europium above CEC.

One of the highlights of this work is that we have succeeded in quantitatively comparing FEBEX and MX-80 in relation to the retention capacity of one key radionuclide. It was found that the differences for the two clays were negligible in this respect, but their retention capacity, either chemical or physical, was lower than that of the reference clay (saponite).

The immobilisation capacity of bentonites through the chemical retention mechanism is also proved and quantified. This impact is highlighted at 300ºC, since at that temperature, the milliequivalents retained were consistently over the CEC. For saponite, the europium reaction is 400-1200% times higher. In FEBEX and MX-80, europium reacts from 130% to 600% (FEBEX), and 130% to 1100% (MX-80) over the CEC. The chemical reaction failed to clearly increase with time for every clay and every temperature. However, in the case of saponite, this increase did remain clear. Since the retention of europium over CEC is a first order kinetical reaction (Alba et al., 2011), it is expected that europium retention in the clays over their CEC capacities (formation of new chemical phases) will be increased with longer reaction times (years).

These results could be critical in HLRW disposal within the engineered barrier, and carry implications towards the stability of the radioactive wastes stored in bentonite since the formation

of chemical phases is expected to be more stable than the sorption in non-specific sites of the clay.

3.2. Reaction rate of Eu^{3+}-clays.

The quantification of the reaction using radioactive ^{152}Eu supports previously found evidence (Alba et al., 2011) that showed a strong dependence of the reacted europium and its reaction velocity on temperature and time.

Figure 2 presents the results for the hydrothermal treatment with the clays at different temperatures. The ratio in the ordinate of Figure 2 represents the ^{152}Eu measured in the solution, (that is, unreacted ^{152}Eu), referring to the total ^{152}Eu collected after the treatment, and was shown versus time. In other words, ^{152}Eu is measured in clay and solution, and the total represents the ^{152}Eu involved in the reaction: reacted (^{152}Eu measured within the clay) and unreacted (^{152}Eu measured in the remaining solution). The europium amount in the remaining solution decreased with time and temperature. The ^{152}Eu concentration in the solution (Fig. 2), which is directly related to europium reactivity, was fitted to an exponential (first order kinetic reaction) with a good regression coefficient, especially for higher temperatures and/or long reaction times (Table 3). The exponent of the fitting provided the reaction velocity constant, *k*, according to

$$I = I_0 e^{-kt} \quad (1)$$

The *k* values obtained from the exponential fitting for saponite, FEBEX, and for MX-80 at various temperatures are displayed in Table 3. From the *k* value, and by taking into account a first-order reaction, the half-life of the reaction ($T_{1/2} = ln2/k$) was calculated and shown in Table 3.

188 The velocity rate (*k*) depends on the temperature. At 350ºC ≤ T≤ 200ºC, the velocity of the
189 reaction was relatively fast and the fitted exponentials showed steep slopes. Their reaction rate
190 constants, *k*, were also similar within the uncertainty (Table 3). *k* values displayed in Table 3, can
191 be used to calculate the half-life of the exponential decay. Which is 49.5 days in this case.
192 According to the definition of half-life at least 5 half-lives are needed to consider that the
193 exponential decay approached approximately zero, i.e. around 8 months would be needed for the
194 total retention of the europium by the saponite.
195 On the other hand, at 150ºC and 80ºC, the decay was slower and longer reaction times were
196 needed in order to evaluate the constant rate accurately; that is why the exponential fitting for
197 150ºC and 80ºC display poorer regression-fitting parameters (R^2 lower than 0.7). An estimation
198 of the reaction constant was obtained for both temperatures, and despite the higher uncertainties,
199 it remains clear that the constant of the exponential fitting was significantly lower. Calculated *k*
200 values were one order of magnitude lower than for T≥ 200ºC (Table 3). Lower *k* values result in
201 longer reaction times (within three years) needed to complete the immobilisation of the
202 europium.
203 It is worth noticing that reaction velocities were classified in two groups of temperature (350-
204 200ºC and 150-80ºC) and provided two distinct *k* values for every group. Within the same
205 temperature, arranged *k* velocities were indistinguishable, in accordance with the uncertainty.
206 Moreover, *k* values quantified in Table 3 were equivalent for the three clays. Within
207 uncertainties, equivalent reaction velocities were observed for saponite, FEBEX and MX-80.
208 This implies that various types of clay affect the concentration of retained europium, but not their
209 reaction velocities. The time needed to complete the reaction is thus independent of the clay. To
210 immobilise all the europium at 300-350ºC, approximately 8-9 months would be needed. The

211 reaction time increases for lower temperatures; to immobilise all the europium at 80-150ºC,
212 several years would be needed.

213 In Alba et al. (2011) it is presented europium reaction with saponite (i.e. europium
214 immobilization by saponite) at 300ºC, 200ºC, 150ºC, and 80ºC. It increases with the temperature
215 and its reaction velocities are discriminated into two groups, according to the temperature. The
216 following relationship was found:

217 $Eu_{reacted}(350ºC) > Eu_{reacted}(200ºC) > Eu_{reacted}(150ºC) > Eu_{reacted}(80ºC)$.

218 Figure 2 shows that for the three clays, the amount of unreacted europium at 300-350ºC was
219 lower than at 150ºC and 80ºC. Furthermore, at 300-350ºC, the amount of retained europium
220 clearly depended on the clay used in the reaction. The following relationship is thereby inferred
221 in terms of capacity of immobilisation of europium at 300ºC.

222 $$Eu_{reacted}(saponite) >> Eu_{reaccted}(FEBEX) > Eu_{reacted}(MX\text{-}80)$$

223 At 80ºC and 150ºC, the trend was similar. At 150ºC, the points were scattered, although
224 saponite provided clearly higher reactivity values, and FEBEX and MX-80 provided
225 indistinguishable reactivity. Values seemed to be higher for MX-80, however this deduction
226 remains inconclusive due to the high uncertainties of the results. At 80ºC, the reactivity was
227 almost equal for all three clays, but could not be verified due to the high dispersion of the results.
228

229 *3.3. Structural studies.*

230 The XRD patterns of the bentonites and those after reaction with $7.9 \cdot 10^{-2}$M $Eu(NO_3)_3$ at
231 300ºC are displayed in Figs. 3b and 4b. The pattern of the original bentonites (Figs. 3a and 4a)
232 show the general and basal reflections. The *hk* bands are composed of asymmetrical reflections
233 with the characteristic "saw-tooth" shape of the two-dimensional reflections (Warren, 1941). The
234 basal reflections are symmetrical. The 14.6 Å and 11.9 Å d_{001} values of unreacted FEBEX and

MX-80 bentonite, respectively, corresponded mainly to the bilayer hydrated Ca^{2+} in the FEBEX interlayer and to the monolayer hydrated Na^{+} in the MX-80 interlayer (Alba et al., 2001; Grim, 1968; Ravina and Low, 1977; Warren, 1941).

After the hydrothermal reaction at 300º C, (Figs. 3 and 4, b-f) the basal spacing of bentonites was increased to 15.5 Å, in agreement with data reported for smectites saturated with multivalent cations (Ravina and Low, 1977). This increase agreed with a sorption of Eu^{3+} equivalent to its CEC at 0 h (see Fig. 1). At reaction times longer than 0 h, where the sorption was higher than the CEC, small reflections in the 10-55º 2θ range were observed as a consequence of the generation of the new phases. In FEBEX, those small reflections corresponded to Eu_2SiO_3 (PDF 35-297, marked with E), quartz (PDF 2-458, marked with q), $Na_8(AlSiO_4)_6(OH)_2$ (PDF 40-0100, marked with a), and $Eu(OH)_3$ (PDF 83-2305, marked with oh). In MX-80, only Eu_2SiO_3 and quartz were detected; the absence of $Eu(OH)_3$ could be due to the final pH value being below 3. The XRD patterns were noisy and showed a prominent background, which indicated the partial disruption of the bentonite framework.

The treatments at 150ºC and 80ºC caused no crystallization of new phases and the unique change in the XRD patterns was the shift of the *001* reflexion towards higher 2θ degree. Figure 5 shows the XRD pattern of both bentonites after hydrothermal treatment at 80ºC for 63 days and at 150ºC for 56 days. In both cases, the 2θ position of the *001* reflection indicates the basal spacing of bentonites, increased up to 15.5 Å, in agreement with the sorption of Eu^{3+} at no specific sites (Ravina and Low, 1977).

These results were corroborated through the compositional mapping by SEM/EDX of the bentonites hydrothermally treated at 150ºC (Fig. 6). In general, the morphology of most of the particles were lamellar with amounts of Si, Al and Eu compatible with bentonites saturated with Eu^{3+} (no specific site sorption), although other compacted particles were observed and were

enriched in Eu. The formation of phases, not observed by XRD, were compatible with $Eu(OH)_3$ or Eu_2SiO_3, and these same phases were observed at 300ºC (specific site sorption and chemical reaction).

Temperature played a greater role than time in the formation of the europium silicate, as is predicted in thermodynamics and kinetics. However, long reaction times are expected to increase the sorption by specific and chemical reaction mechanisms, even for low reaction temperatures.

4. Conclusions

The results demonstrate that two mechanisms are involved in the Eu^{3+}(trivalent actinide chemical analogue) retention by bentonites: sorption in specific and non-specific sites; and chemical reaction within the bentonite framework. These findings have a direct and significant implication in the mechanism of retention of HLRW by the engineered barrier of DGRs: Not only does it increase the immobilisation capacity of the bentonite, but it also increases the expected stability of the radioactive waste stored in bentonite.

Furthermore, the immobilization times can be quantified. The results pointed out that the immobilization of europium by saponite, FEBEX and MX-80 would be completed in 8.5 months at $350º \leq T \leq 200ºC$, whereas several years will be needed at $200º < T \leq 80ºC$.

Acknowledgements.

We are grateful for the financial support from ENRESA (contract nº 0079000121) and from DGICYT and FEDER funds (Projects CTQ2010-14874).

References

Alba, M.D., Becerro, A.I., Castro, M.A., Perdigon, A.C., 2001. Hydrothermal reactivity of Lu-saturated smectites: Part I. A long-range order study. American Mineralogist, 86(1-2): 115-123.

Alba, M.D. et al., 2011. Interaction of Eu-isotopes with saponite as a component of the engineered barrier. Applied Clay Science, 52(3): 253-257.

Alba, M.D., Chain, P., 2005. Interaction between Lu cations and 2 : 1 alumino silicates under hydrothermal treatment. Clays and Clay Minerals, 53(1): 37-44.

Alba, M.D., Chain, P., 2007. Persistence of lutetium disilicate. Applied Geochemistry, 22(1): 192-201.

Alba, M.D., Chain, P., Orta, M.M., 2009a. Chemical reactivity of argillaceous material in engineered barrier Rare earth disilicate formation under subcritical conditions. Applied Clay Science, 43(3-4): 369-375.

Alba, M.D., Chain, P., Orta, M.M., 2009b. Rare-earth disilicate formation under Deep Geological Repository approach conditions. Applied Clay Science, 46(1): 63-68.

Bouby, M., Geckeis, H., Lutzenkirchen, J., Mihai, S., Schafer, T., 2011. Interaction of bentonite colloids with Cs, Eu, Th and U in presence of humic acid: A flow field-flow fractionation study. Geochimica Et Cosmochimica Acta, 75(13): 3866-3880.

ENRESA, 2000. Full-scale Engineered Barriers Experiment for a Deep Geological Repository for High Level Radioactive Waste in Crystalline Host Rock, ENRESA, Madrid.

ENRESA, 2006. Full-scale engineered barriers experiment. Publicación Técnica ENRESA, 05-0/2006, 05-0/2006. ENRESA, Madrid.

Fernandes, M.M., Baeyens, B., Dahn, R., Scheinost, A.C., Bradbury, M.H., 2012. U(VI) sorption on montmorillonite in the absence and presence of carbonate: A macroscopic and microscopic study. Geochimica Et Cosmochimica Acta, 93: 262-277.

Galunin, E., Alba, M.D., Santos, M.J., Abrao, T., Vidal, M., 2010. Lanthanide sorption on smectitic clays in presence of cement leachates. Geochimica Et Cosmochimica Acta, 74(3): 862-875.

Grim, R.E., 1968. Clay Mineralogy. McGraw-Hill Book Company, New York.

Hurtado, S., Villa, M., 2010. An intercomparison of Monte Carlo codes used for in-situ gamma-ray spectrometry. Radiation Measurements, 45(8): 923-927.

Madsen, F.T., 1998. Clay mineralogical investigations related to nuclear waste disposal. Clay Minerals, 33(1): 109-129.

Miller, A.W., Wang, Y.F., 2012. Radionuclide Interaction with Clays in Dilute and Heavily Compacted Systems: A Critical Review. Environmental Science & Technology, 46(4): 1981-1994.

Perdigón, A.C., 2002. Estudio del sistema saponita/Lu(NO3)3/H2O en condiciones hidrotérmicas, University of Sevilla, Spain.

Pusch, R., 2006. Engineered barriers. In: Pusch, V.P.a.R. (Ed.), Disposal of Hazardous Waste in Underground Mines. Wessex Institute of Technology, UK, pp. 35–40.

Ravina, I., Low, P.F., 1977. Change of B-Dimension with Swelling of Montmorillonite. Clays and Clay Minerals, 25(3): 201-204.

Savage, D., Chapman, N.A., 1982. Hydrothermal Behavior of Simulated Waste Glass and Waste Rock Interactions under Repository Conditions. Chemical Geology, 36: 59-86.

Sorieul, S. et al., 2008. Radiation-Stability of Smectite. Environmental Science & Technology, 42(22): 8407-8411.

Stumpf, T., Bauer, A., Coppin, F., Il Kim, J., 2001. Time-resolved laser fluorescence spectroscopy study of the sorption of Cm(III) onto smectite and kaolinite. Environmental Science & Technology, 35(18): 3691-3694.

Trillo, J.M. et al., 1994. Interaction of Multivalent Cations with Layered Clays - Generation of Lutetium Disilicate Upon Hydrothermal Treatment of Lu-Montmorillonite. Inorganic Chemistry, 33(18): 3861-3862.

Villar, M.V., Gómez-Espina, R., Gutiérrez-Nebot, L., 2012. Basal spacings of smectites in compacted bentonite. Applied Clay Science, 65-66: 95-105.

Warren, B.E., 1941. X-ray diffraction in random layer lattices. Physical Review, 59(9): 693-698.

Table 1. Characteristics of the clays selected

Clays	Structural formula	Total charge/ u.c.	CEC[d] (meq/100g)
FEBEX[a]	$(Ca_{0.5}Na_{0.08}K_{0.11})(Si_{7.78}Al_{0.22})(Al_{2.78}Fe^{III}_{0.33}Fe^{II}_{0.02}Mg_{0.81})O_{20}(OH)_4$	1.19	158.2
MX-80[b]	$(Na_{0.36}Ca_{0.20})(Si_{7.96}Al_{0.04})(Al_{3.1}Mg_{0.56}Fe^{III}_{0.18}Fe^{II}_{0.16})O_{20}(OH)_4$	0.76	102.1
Saponite[c]	$Na_{0.8}(Si_{7.2}Al_{0.8})(Mg_{5.79}Fe_{0.14})O_{20}(OH)_4$	0.80	103.0

[a] ENRESA, Spain

[b] CIEMAT, Spain

[c] Source Clays Repository of the Clay Minerals Society, University of Missouri, Columbia, USA

[d]theoretical cation exchange capacity value, mathematically deduced from clay molecular formula

342

Table 2. Temperatures and times used in the hydrothermal treatments with FEBEX and MX-80 bentonite and europium. Stripes correspond to solutions where no radioactive tracer was added

T (ºC)	Time (days)								
	0	2.2	4.5	9	28	35	56	63	120
80									
150									
300									

Table 3. Kinetics parameters of the europium sorption by clays.

T (ºC)	saponite	FEBEX	MX-80
	$k \cdot 10^{-3}$ ($days^{-1}$)		
350	14 ± 5		
300		14 ± 3	11 ± 6
200	11.9 ± 0.1		
150	3.6 ± 1.5	3 ± 1	1.5 ±1.2
80	2.4 ± 2.0	1.0 ± 0.1	2 ± 1
T(ºC)	$T_{1/2}$ (days)		
350	50 ± 2		
300		50 ± 10	60 ± 30
200	58.2 ± 0.5		
150	190 ± 80	230 ± 80	460 ±300
80	290 ± 240	690 ± 70	350 ± 170
T(ºC)	Regression coefficient (R^2)		
350	0.9959		
300		0.7669	0.6598
200	0.9951		
150	0.2912	0.9708	0.8770
80	0.4453	0.9826	0.0961

Figure Captions

Fig. 1. Amount of stable europium retained in the solid phase in FEBEX, MX-80 and saponite. The solid line indicates the CEC of FEBEX, and the dashed line the CEC of MX-80 and saponite. Red columns correspond to FEBEX results, blue columns correspond to MX-80 and the grid pattern corresponds to saponite. Blank results mean that no experiment was performed for that reaction time.

Fig. 2. ^{152}Eu (Bq) in the liquid phase after the hydrothermal treatment (unreacted ^{152}Eu) with saponite, FEBEX and MX-80 versus time at (a) 300 °C, (b) 150 °C, and (c) 80 °C, data were fitted to an exponential function. Initial ^{152}Eu added was 9 Bq. Red corresponds to FEBEX results, blue to MX-80, and black to saponite.

Fig. 3. XRD diagrams of bentonite FEBEX: (a) before treatment; (b) after the hydrothermal treatments at 300 º C for 0 h; (c) for 2.25 days; (d) for 4.5 days; (e) for 9 days; and (f) for 11 days. E=$EuSiO_3$ (PDF 35-297), oh=$Eu(OH)_3$ (PDF 83-2305), a=$Na_8(AlSiO_4)_6(OH)_2$ (PDF 40-0100) and q=quartz (PDF 2-458).

Fig. 4. XRD diagrams of bentonite MX-80: (a) before treatment; (b) after the hydrothermal treatments at 300 º C for 0 h; (c) for 2.25 days; (d) for 4.5 days; and (e) for 9 days. E=$EuSiO_3$ (PDF 35-297) and q=quartz (PDF 2-458).

Fig. 5. XRD diagrams of bentonite FEBEX (left) and bentonite MX-80 (right): (a) before treatment; (b) after the hydrothermal treatments at 80º C for 63 days; and (c) at 150º C for 56 days.

Fig. 6. SEM/EDX of bentonite FEBEX (left) and MX-80 (right) after hydrothermal treatment at 150º C for 28 days.

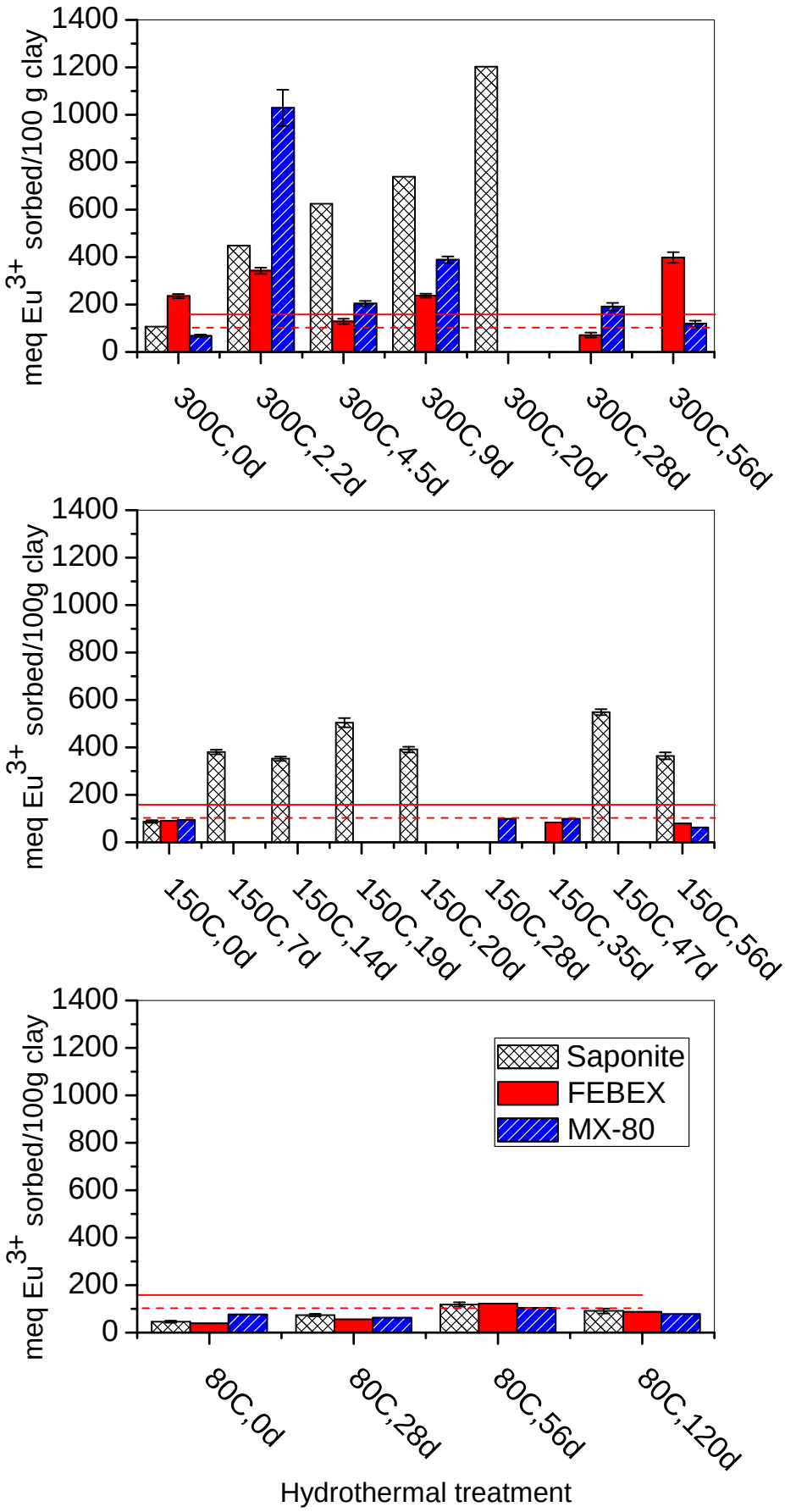
meq Eu3+ sorbed/100 g clay
meq Eu3+ sorbed/100g clay
meq Eu3+ sorbed/100g clay
0
200
400
600
800
1000
1200
1400
300C,0d
300C,2.2d
300C,4.5d
300C,9d
300C,20d
300C,28d
300C,56d
150C,0d
150C,7d
150C,14d
150C,19d
150C,20d
150C,28d
150C,35d
150C,47d
150C,56d
80C,0d
80C,28d
80C,56d
80C,120d
Saponite
FEBEX
MX-80
Hydrothermal treatment

371 *Figure 1*

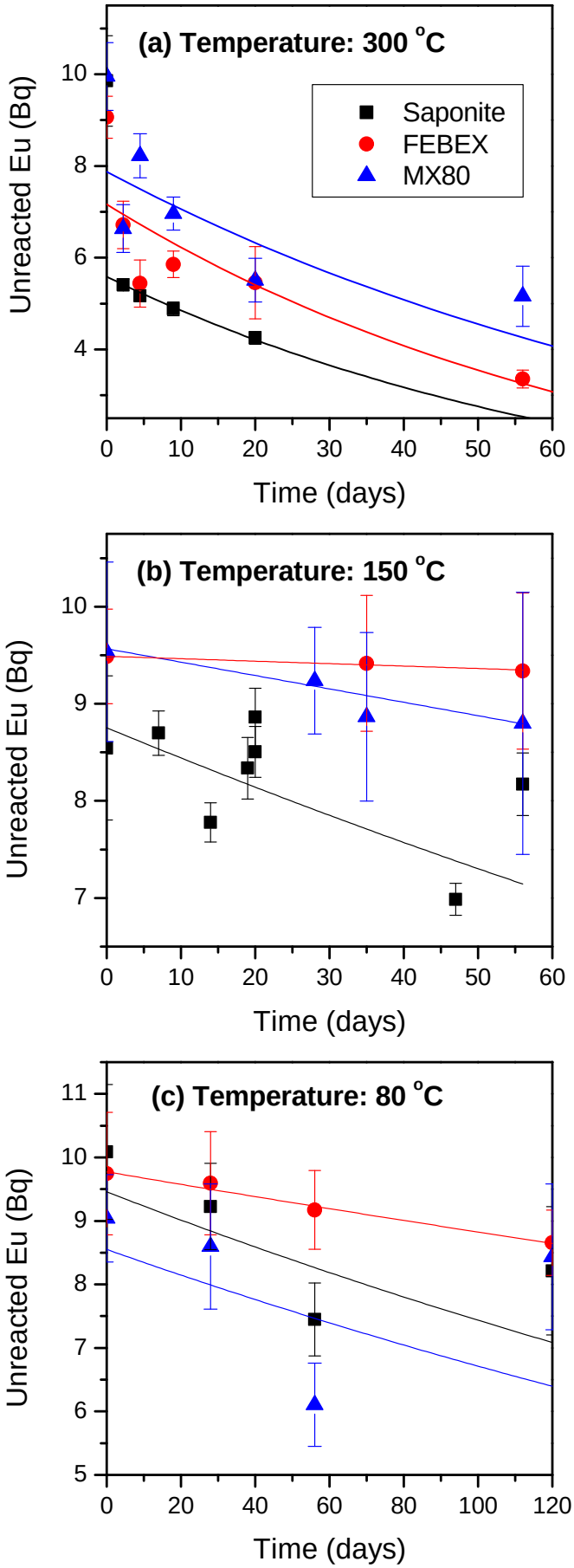
(a) Temperature: 300 °C
Saponite
FEBEX
MX80
Unreacted Eu (Bq)
Time (days)
(b) Temperature: 150 °C
Unreacted Eu (Bq)
Time (days)
(c) Temperature: 80 °C
Unreacted Eu (Bq)
Time (days)

372 *Figure 2*

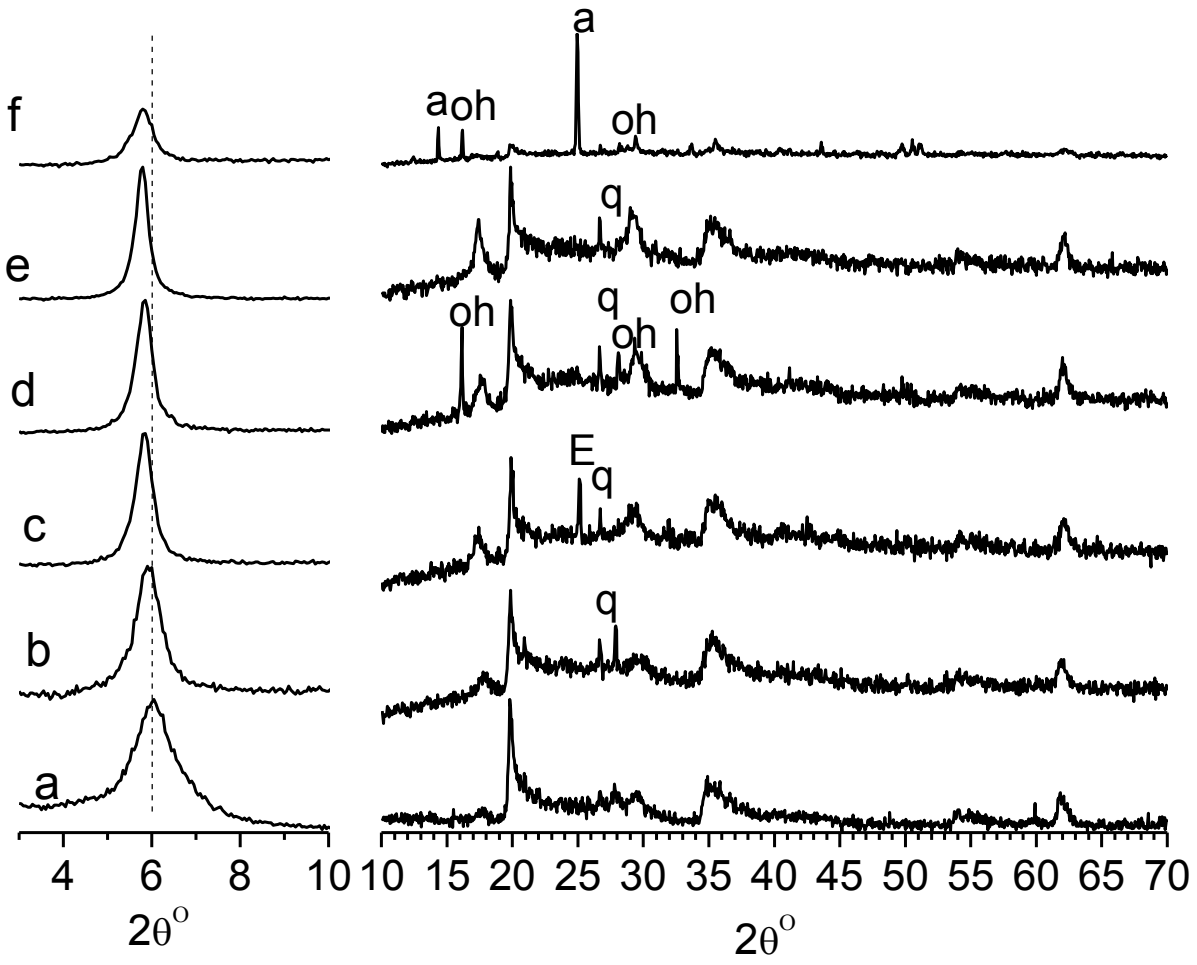
a
aoh
oh
f
q
e
oh
q
oh
oh
d
E
q
c
q
b
a
4
6
8
10
2θ^O
10
15
20
25
30
35
40
45
50
55
60
65
70
2θ^O

Figure 3

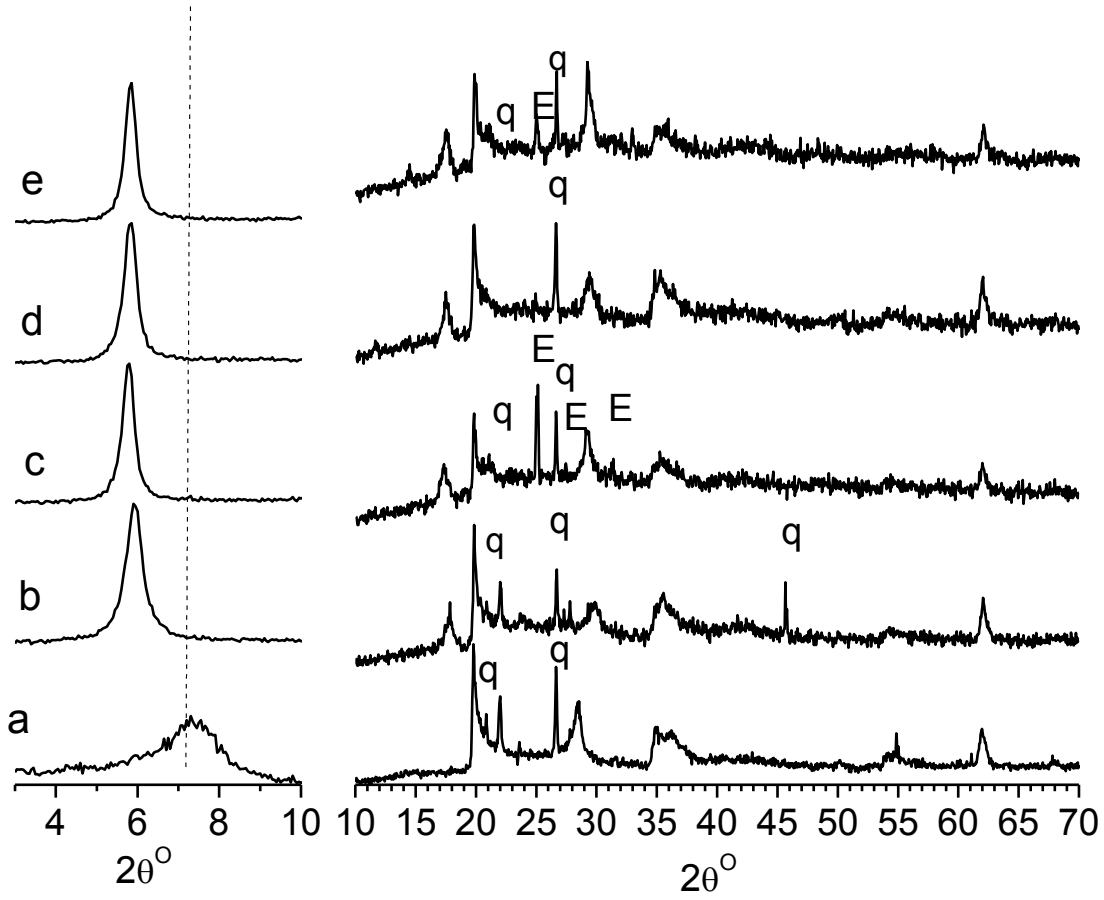

382

383

384 *Figure 4*

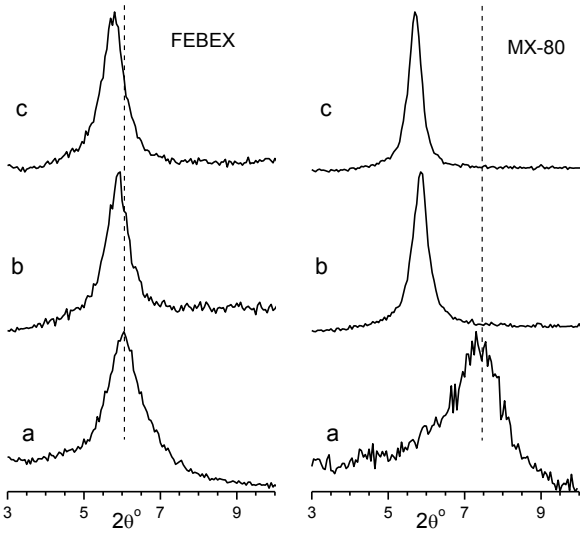

385 *Figure 5*

386

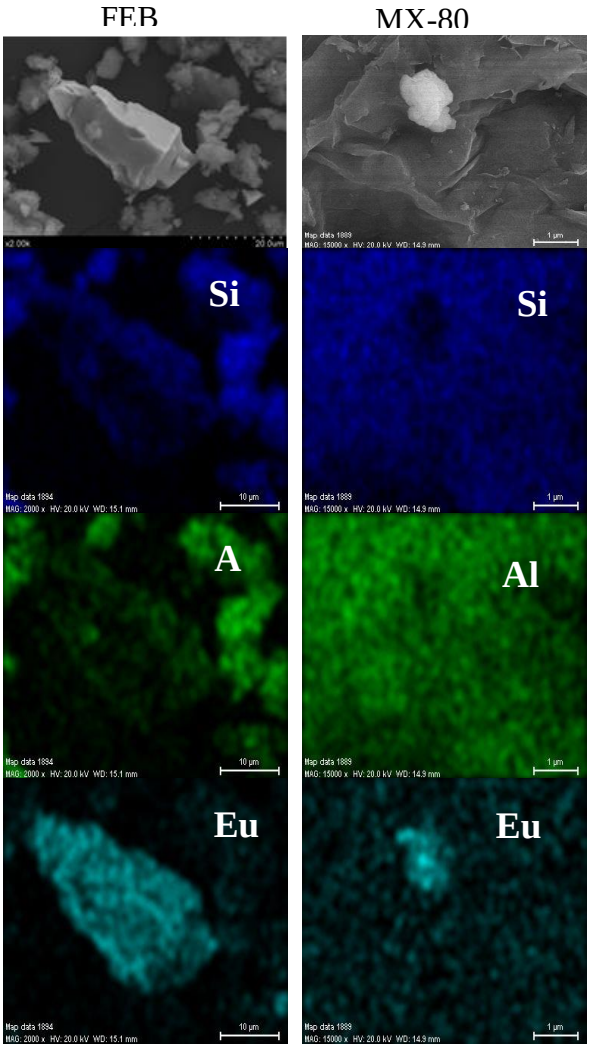

387

388

389 *Figure 6*

390